

BENCHMARK OF SUPERCONDUCTING CAVITY MODELS AT SNS LINAC*

A. Shishlo†, Oak Ridge National Laboratory, Oak Ridge TN, USA

Abstract

A benchmark of superconducting cavity models against Time-of-Flight measurements at the SNS linac is presented. The superconducting part of the SNS linac (SCL) includes 81 RF cavities that accelerate H⁻ beam from 185.6 MeV to the final energy of 1 GeV. During operation some of the cavities can become unstable, and the corresponding amplitudes should be reduced, or the cavities should be completely switched off. In this case, the SCL is retuned by using a linac simulation code. This simulation tool relies on the accuracy of the superconducting cavity model. This paper describes the comparison of the measured beam acceleration by one of the SCL cavities and simulations of this process. Different cavity models are used in the simulations. The subject of this study is limited to longitudinal beam dynamics, so no effects on transverse beam characteristics have been considered.

INTRODUCTION

Superconducting radiofrequency (RF) structures have become preferred choices for high power linacs. The physical models describing these accelerating cavities are important not only for the design but also for operational practices of these linacs. This paper describes an attempt to benchmark two models of RF cavities used at the Spallation Neutron Source (SNS) superconducting linac (SCL).

The SNS is a user facility, so high availability is a key factor in the SNS operations. This means that any production interruptions should be minimised including any adjustments in the superconducting linac. The adjustments related to SCL cavities should be followed by retuning of the linac to keep the output energy the same and to avoid subsequent SNS ring and transport lines retuning. Nowadays all SCL retuning is done very fast by using the OpenXAL online model [1, 2]. Usually, the deviation of the final energy from the requested value after retuning does not exceed 1.5 – 2 MeV on top of about 1 GeV. Although this is a satisfactory outcome, it is an open question if we can improve the model-based tuning with a better cavity model. Here we present a first attempt to benchmark the models of superconducting cavities implemented in the PyORBIT code [3]. These models are slightly different from the one implemented in OpenXAL. They are described in [4], and eventually we plan to use them in the SNS operations.

* This manuscript has been authored by UT-Battelle, LLC, under Contract No. DE-AC05-00OR22725 with the U.S. Department of Energy. The United States Government retains, and the publisher, by accepting the article for publication, acknowledges that the United States Government retains a non-exclusive, paid-up, irrevocable, world-wide license to publish or reproduce the published form of this manuscript, or allow others to do so, for United States Government purposes. The Department of Energy will provide public access to these results of federally sponsored research in accordance with the DOE Public Access Plan.

† shishlo@ornl.gov

BENCHMARK PROCEDURE

The SNS SCL consists of 81 superconducting cavities enclosed in 23 cryo-modules. There are two types of cavities: medium and high-beta cavities with geometries providing maximal acceleration efficiencies for two ranges of the beam energies, from 186 to 400 MeV and from 400 to 1000 MeV. For the benchmark, we chose a cavity from the last medium-beta cryo-module – Cav11a to cover wide range of the relativistic parameter beta of the incoming beam.

Measurements

For the benchmark we switched off all downstream cavities and created five settings for upstream cavities that gave us five different energies from 200 to 400 MeV with longitudinally focused bunches at the Cav11a entrance. For each of the settings we collected statistics of Beam Position Monitor (BPM) signals with Cav11a off to get the precise initial energy at the cavity entrance and results of cavity phase scans. In addition to the beam transverse position inside the beam pipe, the SNS linac BPMs deliver arrival phase and amplitude of the particle bunch. The phase is proportional to the bunch travel time, and the amplitude signal is proportional to the amplitude of a first Fourier harmonic of the bunch longitudinal density distribution. We used these amplitude BPM signals to make bunches as short as possible at the cavity entrance for all five configurations. For all measurements we used a very short beam pulse of 0.5 μ s to avoid beam loading. For all cases we did not change the cavity field gradient.

Cavity Models

The SNS linac superconducting cavity from the medium beta section is shown in Fig. 1. It has 6 accelerating RF gaps and an equivalent length 68.2 cm. The design peak gradient of electric field is 27.5 MV/m, and the frequency is 805.0 MHz.



Figure 1: SNS linac superconducting cavity.

During the analysis we used 2 models of this RF cavity. The first model represents the cavity as a zero-length lattice

element that changes the energy of the particle according to Panofsky's equation

$$\Delta W = E_0 TL \cdot \cos(\phi_{cav} + \phi_{cav}^{(offset)}) \quad (1)$$

In this model the phase of the particle does not change after passing through the cavity. We call this a "simplified" model.

The second model has 6 RF accelerating gaps with unique symmetrical and asymmetrical transit-time factors [4]. These transit-time factors were calculated from the simulated electric field distribution along the cavity z-axis. We consider this model to be more realistic than the first one.

Analysis

The analysis part of the benchmark includes three stages. First, we analyze the downstream BPM phase statistics with the RF cavity off to calculate the energy at the entrance of the cavity. On the second stage, the model-independent analysis of the cavity phase scan is performed. We changed cavity phase from -180 to +180 with 5 degree steps. For each cavity phase we got all BPM phases which also allows us to calculate the energy of the beam after the cavity. On the third stage we extracted the cavity model parameters (cavity amplitude and phase offset relative to the RF signal distribution line) by fitting measured and calculated BPM phases for each cavity phase point.

The analysis, as we can see, has a model-independent component, and we will start with these results.

MODEL INDEPENDENT RESULTS

The analysis started with the calculated initial energies by using the BPM phases downstream of the switched off Cav11a. The analysis was performed according to the algorithm described in [5]. The BPM phase offsets from the RF distribution line were defined from the ring energy measurements also described in [5]. The set of kinetic energies and their errors at the Cav11a entrance are specified in Table 1. The errors are defined by the BPM phase statistics.

Table 1: Initial Kinetic Energies

Case #	E_{kin} , MeV	E_{kin} Error, MeV
1	213.524	0.008
2	262.842	0.009
3	315.664	0.009
4	368.891	0.008
5	412.963	0.009

Plots in Fig. 2 show the BPM phases, errors, and the linear fit along the SCL linac starting from BPM10 that is right before Cav11a and up to BPM21 which is 85 meters downstream. Phases for each BPM were adjusted by the BPM phase offset (fixed for all cases) and $360 \cdot n$ deg to get an almost straight line. The slope of the linear fit defines

the initial energy for the case 1 in Table 1, and data for all other energies are similar. The plots show that on top of 80000 deg phase advance from the BPM10 we have deviations from the fit of about 1 deg, and it is possible that all average values of these deviations are zero.

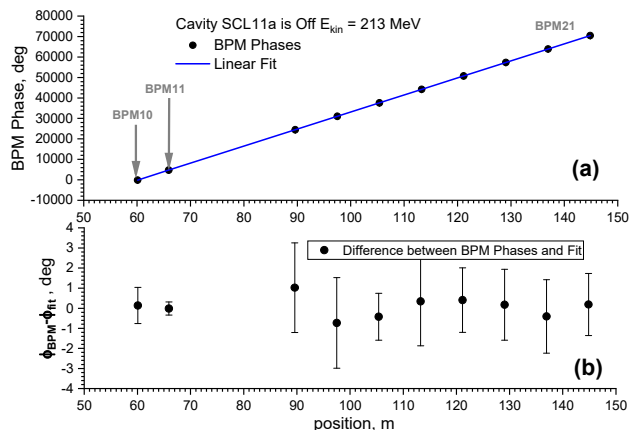


Figure 2: (a) phases of BPMs and linear fit (b) difference between phases and fit values.

Similar fitting procedures were performed for each cavity phase for all initial energies. As results we got output energies vs. cavity phase dependencies. One of these is shown in Fig. 3 for the input kinetic energy 213 MeV. These data are also model-independent and can be used for controlling the quality of the models, but they do not account for the time the synchronous particle spends moving inside the cavity. Therefore, we will use the BPM phase data for completeness.

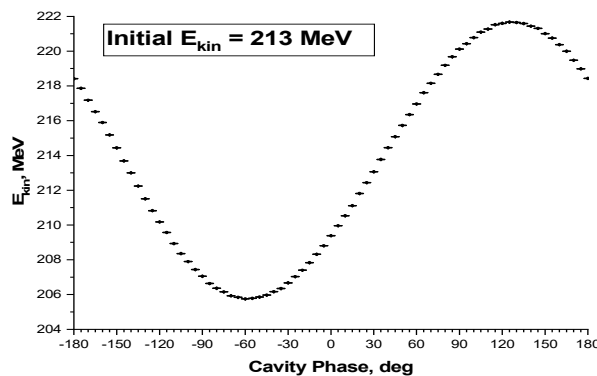


Figure 3: Output energy vs. cavity phase.

Another interesting model-independent representation of the phase scan data is a set of linear fits of BPM phases (like the line shown in Fig. 2a) for all cavity phase values in one plot. All these fitted lines should cross approximately at one point near the center of the cavity. To make it clearer we subtracted from each fitted line the fitted line for the "cavity off" statistics (Fig. 2a for Case 1 in Table 1), and we put them on the plot for positions near the center of the cavity. This plot is shown in Fig. 4. Using the pair-wise positions of these lines crossing, we calculated an average position for all initial energies as 61.594 ± 0.014 . This value exceeds the value that we have in our linac lattice file by

3.2 cm. This difference is almost inside our accuracy, but it will be shown later that it is a correct value from the point of view of the combined BPMs and the cavity phase analysis.

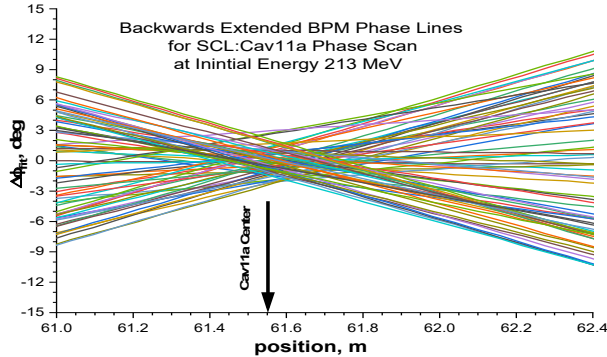


Figure 4: BPM fitted lines for each cavity phase point during the phase scan (see text for explanation).

FITTED PARAMETERS OF MODELS

The parameters of the simplified and the 6 RF gap models were defined by fitting the whole array of BPM phases for each of the cavity phase scans. As an example, the results of fitting for the initial energy 213 MeV and the simplified model are shown in Fig. 5 for two BPMs. The last BPM is 90 m downstream of the cavity. Figure 5 demonstrates that the simplified model cannot reproduce the second harmonics of the BPM phase function. This is not a surprise considering the Eq. (1).

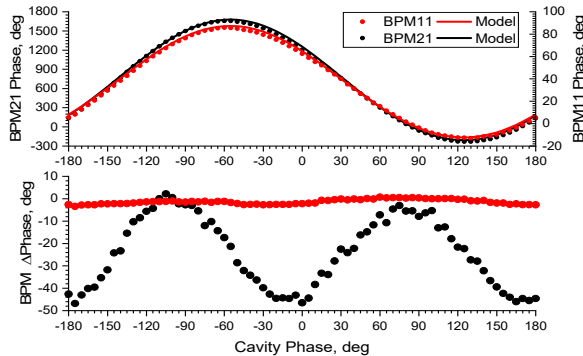


Figure 5: BPM phases vs the cavity phases during the scan. Simplified model and data comparison.

The corresponding plot for the 6 gap cavity model is shown in Fig. 6. This model gives much better agreement with data.

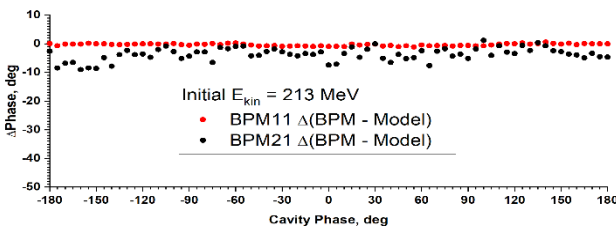


Figure 6: The 6 gap model and BPM data difference.

One set of results of the fittings for both models are cavity amplitudes for all five initial energies. These amplitudes should be the same for all cases. These amplitudes, shown in Table 2, are not constant for both models, and the calibration accuracy of amplitudes of our cavities is about 2% if we consider all initial energies.

Table 2: Amplitudes of Cavity for Both Models. E0L ss for the Simplified and A is for 6 Gap Models

E_{kin} , MeV	E_{0L} , MV	A , Arb. Unit
213	13.14 (+2.0%)	1.294 (+2.4%)
263	13.10 (+1.7%)	1.288 (+1.9%)
316t	13.02 (+1.1%)	1.281 (+1.3%)
369	13.04 (+1.2%)	1.283 (+1.4%)
413	12.88 (+0.0%)	1.264 (+0.0%)

The analysis of the output energies in the cavity phase scan showed that we can predict the energy with accuracy about 150 keV for the simplified model and to within 80 keV for the more accurate 6 gap model.

As for cavity phase offsets analysis, we found that they are related to the beam arrival time (from BPM phase analysis) at the center of the cavity by a formula

$$\phi_{cav}^{(offset)} - 2 \cdot \phi_{BPM} = const \quad (2)$$

The coefficient 2 in this equation is the result of frequencies ratio for BPM (402.5 MHz) and SCL cavities RF systems (805 MHz). The accuracy of the constant in Eq. (2) is about 0.5 deg if we move the cavity position in the models 3.1 cm downstream, and it is 5 deg otherwise.

CONCLUSION

We can consider this benchmark to be successful because the agreement between even the simplified model and data gives us a firm confidence that we can use this model for the SCL retuning. The reasons for that are small changes in the entrance energies during the retuning process, small distances between cavities and small errors in the predicted output energies which do not allow big errors in the arrival phases at the next cavity. However, there is a discrepancy between the models and data which needs further analysis. This analysis should include the replacement of a single particle model with a multi-particle bunch, a closer look at the cavity model itself, and error analysis of the model parameters.

REFERENCES

- [1] Openxal, <https://github.com/openxal/openxal>
- [2] J. Galambos *et al.*, "XAL Application Programming Structure", in *Proc. 2005 Particle Accelerator Conf. (PAC'05)*, Knoxville, Tennessee, USA, May 2005. pp. 79-83. doi:10.1109/pac.2005.1590365
- [3] PyORBIT-Collaboration, <https://github.com/PyORBIT-Collaboration>

- [4] A. Shishlo and J. Holmes, "Physical Models for Particle Tracking Simulations in the RF Gap", Preprint ORNL/TM-2015/247, Jun. 2015.
- [5] J. C. Wong *et al.*, "Laser-assisted charge exchange as an atomic yardstick for proton beam energy measurement and phase probe calibration," *Phys. Rev. Accel. Beams*, vol. 24, p. 032801, Mar. 2021.
doi:10.1103/physrevaccelbeams.24.032801